

Influence of earthquake record truncation on fragility curves of RC frames with different damage indices



Alireza Khaloo^a, Saeed Nozhati^a, Hassan Masoomi^a, Hadi Faghihmaleki^{b,*}

^a Department of Civil Engineering, Sharif University of Technology, Tehran, Iran

^b Department of Civil Engineering, Babol Noshirvani University of Technology, Babol, Iran

ARTICLE INFO

Article history:

Received 5 January 2016

Received in revised form

8 May 2016

Accepted 10 May 2016

Available online 10 May 2016

Keywords:

Ground motion duration

Truncation

RC frame

Incremental dynamic analysis

Fragility curves

ABSTRACT

Probabilistic seismic analysis of structures with incremental dynamic analysis (IDA) is a widely used method to offer comprehensive evaluation of the seismic performance of structures. Although IDA is a powerful computer-intensive method, it is really a time-consuming procedure. Accordingly, in this study, for coping with this problem, significant motion duration is used instead of total motion duration. This truncation can significantly reduce the computational effort and time. In order to determine the influence of truncation, fragility curves and their mean annual frequencies (MAF) in each limit state are used with two different damage indices, namely modified Park & Ang and maximum inter-story drift, for different RC frames. Although truncation can produce larger errors in fragility curves of high-rise structures and different structures with energy-based or combination indices because of their greater dependence on record duration, this study has shown that it causes negligible errors in fragility curves of mid-rise structures with deformation-based indices.

© 2016 Elsevier Ltd. All rights reserved.

1. Introduction

Engineers have been seeking more accurate modeling and investigating of structures under earthquake excitations, and modeling software is constantly developing. Thereby, nowadays, non-linear modeling and analysis of structures are not really difficult. Incremental dynamic analysis is one of the most powerful analyses, which is used for investigating seismic performance of structures. Although this is a widely applicable method and it can present a lot of precise information about structures, it is really time-consuming, and state-of-the-art computers are needed for investigation of massive structures. All researchers have been seeking efficient methods and software by which they can increase the speed of analyses; thereby, they can obtain more precise outputs during less spending of time.

IDA has been used by several researchers for different studies. For example, Mander et al. [1] used it for seismic risk assessment of bridges; Pinho et al. [2] used it to evaluate the accuracy of static pushover methods on twelve bridges, and Goulet et al. [3] relied on IDA to estimate seismic losses for a reinforced concrete frame structure.

Inasmuch as IDA is a widely used method for assessing structural performance in recent decades, many researchers have been

trying to improve the performance of IDA, and they have presented efficient methods, such as IM selection [4] progressive IDA for first-mode dominated structures [5], use of a trilinear idealization model of IDA for RC structures [6], and implementation of IDA in parallel [7]. As mentioned above, although IDA is really a widely applicable method, it is time-consuming; hence, in this study, strong motion duration is used instead of total motion duration.

Although the effect of ground motion duration on liquefaction and slope stability is recognized, its influence on structural response and fragility curves is a debatable topic. Some researchers, such as Ruiz-Garcia [8], Iervolino [9], Raghunandan and Liel [10], have studied on the influence of motion duration, and they indicated that the longer duration record proves more damage to the structure than shorter duration record because the longer duration ground motion imposes high energy demands on the structure. In this regard, most of them considered two different ground motions, whereas in this research one set of ground motion with different motion duration is considered.

2. Model and ground motion record selection

Three different types of intermediate moment RC frame systems, which have 5, 10, 20 stories (Fig. 1) were modeled for considering whether maximum response of structure occurs in strong motion duration or not. These frames are assumed to be located in

* Corresponding author.

E-mail address: h.faghihmaleki@gmail.com (H. Faghihmaleki).

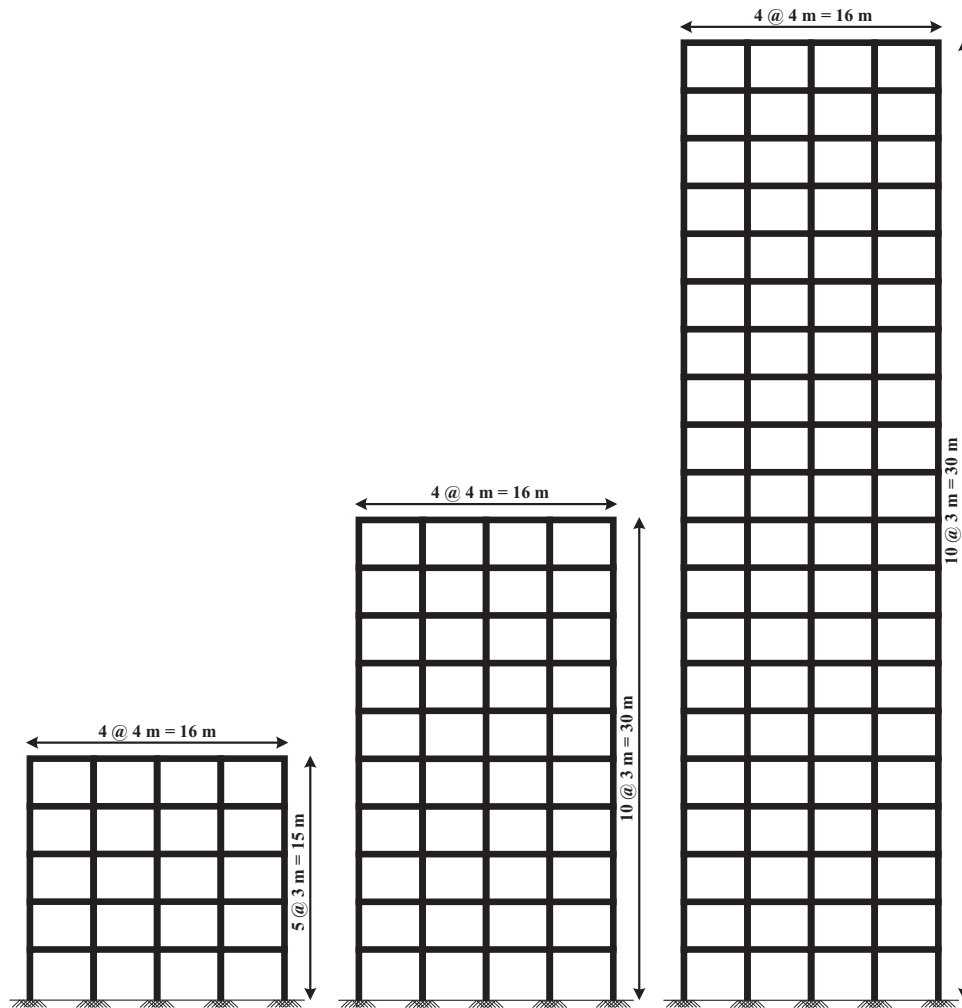


Fig. 1. View of studied frames.

Table 1

The suite of twenty ground motion records used.

Earthquake name	Station name	Magnitude (Ms)	Component (deg.)	PGA (cm/s ²)
Imperial Valley, 1979	El Centro, Parachute Test Facility	6.8	315	200.2
San Fernando, 1971	Pasadena, CIT Athenaeum	6.5	90	107.9
San Fernando, 1972	Pearblossom Pump	6.5	21	133.4
Landers, 1992	Yermo, Fire Station	7.5	0	167.8
Loma Prieta, 1989	APEEL 7, Pulgas	7.1	0	153
Loma Prieta, 1990	Gilroy #6, San YsidroMicrowavv Site	7.1	90	166.9
Loma Prieta, 1990	Saratoga, Aloha Ave	7.1	0	494.5
Loma Prieta, 1990	Gilroy, Gavilon College PhysSchBldg	7.1	67	349.1
Loma Prieta, 1990	Santa Cruz, University of California	7.1	360	433.1
Loma Prieta, 1990	San Francisco, Dimond Heights	7.1	90	110.8
Loma Prieta, 1990	Fremont, Mission San Jose	7.1	0	121.6
Loma Prieta, 1990	Monterey, City Hall	7.1	0	71.6
Loma Prieta, 1990	Yerba Buena Island	7.1	90	66.7
Loma Prieta, 1990	Anderson Dam, Downstream	7.1	270	239.4
Morgan Hill, 1984	Gilroy, Gavilon College PhysSciBldg	6.1	67	95
Morgan Hill, 1984	Gilroy #6, San YsidroMicrowavv Site	6.1	90	280.4
Palmsprings, 1986	Fun Valley	6	45	129
Northridge, 1994	Littlerock, Brainard Canyon	6.8	90	70.6
Northridge, 1994	Castaic, Old Ridge Route	6.8	360	504.2
Northridge, 1994	Lake Hughes #1, Fire station #78	6.8	0	84.9

the seismicity zone II of the 4 zones system specified by Iranian standard 2800 [11] and are therefore designed respectively for seismic base shears of 12%, 8.5%, 6% of their seismic weights. The first periods of 5, 10 and 20 story frames are 0.48, 0.96 and 1.56 s respectively.

The analyses of the buildings are conducted using the finite element software SeismoStruct [12], which is capable of calculating the large displacement behavior of space frames under static or dynamic loading, taking into account both geometric nonlinearities and material inelasticity. The spread of material

Table 2
 Significant and other important parameters of each Earthquake record.

EQ. name	Tr (s)	t ₁	t ₂	Significant duration (s)	Arias intensity (m/sec) – original record	Arias Intensity (m/sec) – truncated record	CAV (cm/sec) – original record	CAV (cm/sec) – truncated record
Imperial Valley, 1979	39.325	6.92	23.78	16.86	0.220	0.198	432.34	314.76
San Fernando, 1971	28.48	5.42	17.74	12.32	0.209	0.188	382.31	293.94
San Fernando, 1972	27.25	0.94	14.58	13.64	0.248	0.223	421.076	333.57
Landers, 1992	49.98	6.3	38.08	31.78	0.7066	0.636	1071.78	864.57
Loma Prieta, 1989	39.94	5.645	20.32	14.68	0.289	0.260	490.98	353.35
Loma Prieta, 1990	39.94	3.49	16.11	12.62	0.442	0.397	554.57	392.64
Loma Prieta, 1990	39.94	4.635	13.99	9.36	1.451	1.30	911.25	610.55
Loma Prieta, 1990	39.94	2.805	7.8	5.0	0.903	0.811	587.17	359.89
Loma Prieta, 1990	39.94	5.555	23.93	18.37	0.102	0.092	312.63	228.04
Loma Prieta, 1990	39.94	8.19	17.465	9.275	0.104	0.09358	243.8	163.642
Loma Prieta, 1990	39.94	6.685	24.86	18.18	0.268	0.241	527.4	388.046
Loma Prieta, 1990	39.94	4.05	14.735	10.685	1.236	1.112	888.36	600.087
Loma Prieta, 1990	39.94	2.365	9.24	6.875	3.237	2.89	1248.7	844.41
Loma Prieta, 1990	39.59	4.31	14.82	10.51	0.796	0.716	714.87	505.438
Morgan Hill, 1984	29.97	1.03	9.6	8.57	0.0566	0.0508	170.1	125.077
Morgan Hill, 1984	29.97	1.59	8.055	6.425	0.870	0.7825	604.97	417.115
Palmsprings, 1986	20.13	1.48	11.745	10.265	0.133	0.119	270.21	209.14
Northridge, 1994	39.94	3.36	13.2	9.84	1.794	0.41	1038.13	184.22
Northridge, 1994	39.94	5.46	14.54	9.08	2.787	1.256	1305.34	425.77
Northridge, 1994	31.96	4.2	16.94	12.74	0.0375	0.033	161.9	114.535

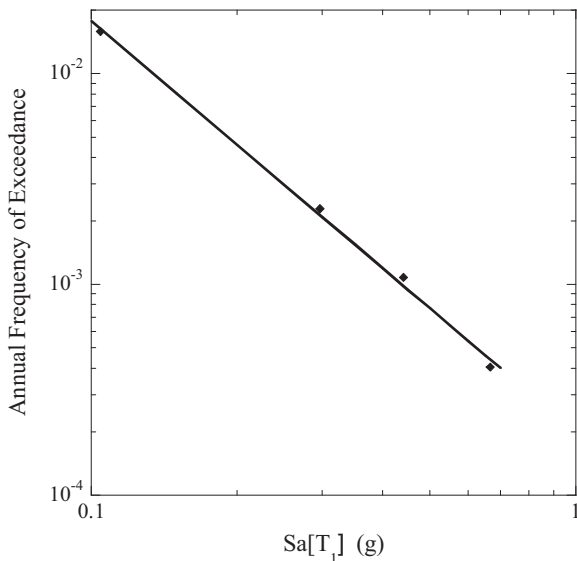


Fig. 2. Seismic hazard curve of the central region of Tehran in the logarithmic scale.

inelasticity along the member length and across the section area is represented through the employment of a fiber-based modeling approach, implicit in the formulation of SeismoStruct’s inelastic beam-column frame elements. Thus, the sectional stress-strain state of beam-column elements is obtained through the integration of them on linear uniaxial material response of the individual fibers in which the section is subdivided. For the present analysis, the frame sections are divided into 100 fibers. Distributed inelasticity frame elements are implemented assuming force-based (FB) formulations and considering 4 controlling integration sections along the element.

Concrete was modeled by using a uniaxial constant-confinement model based on the constitutive relationship proposed by Mander [13] and later modified by Martinez-Rueda and Elnashai [14] to cope with some problems concerning numerical stability under large displacements. The confinement effects, provided by the transverse reinforcement, were taken care of as proposed by Mander, whereby a constant confining pressure was assumed in the entire stress-strain range. The model required the introduction

of 4 parameters: the compressive and tensile strengths of the unconfined concrete (were considered respectively 25 MPa, 0 MPa), the crushing strain (0.002) and the confinement factor defined as the ratio between the confined and unconfined compressive stress of the concrete (1.2). The steel stress-strain relationship is based on behavior proposed by Menegotto [15] steel model and modified by Filippou et al. [16] and Fragiadakis [17] and yield strength equal to 400 MPa are adopted.

Earthquake ground motion records, which were used in this research are set twenty earthquakes selected from FEMA440 [18] Recorded on Site Class C; These records have relatively similar shear velocity and response spectrum in comparison to soil type II specified by Iranian standard 2800. By considering 20 different ground motions, record to record variability is considered. These ground motion records are listed in Table 1.

3. Ground motion duration

A ground motion time history of definite earthquake at a definite site can be characterized by a number of parameters including amplitude, frequency content, energy, and duration of shaking. There are many definitions for ground motion duration [19]. The bracketed duration considers the amplitude of the ground motion to measure the duration and is defined as the length of the time between which the absolute accelerogram exceeds some threshold acceleration for the first and last time. The significant duration, on the other hand, is defined based on the energy of the ground motion record. Several measures serve as proxies for the total energy of the accelerogram, including the integral of the square of the acceleration history over time $a(t)$, which is known as the Arias Intensity (AI) and is calculated as:

$$AI = \frac{\pi}{2g} \int_0^{T_r} a^2(t) dt \quad (1)$$

where T_r is the total duration of the accelerogram, and g is the gravity acceleration. Among the different definitions of significant duration, the 5–95% significant duration [20] is used here, as it has been in a number of other studies [21]. The 5–95% significant duration, is calculated as the interval between the times at which 5% and 95% of the Arias Intensity of the ground motion has been

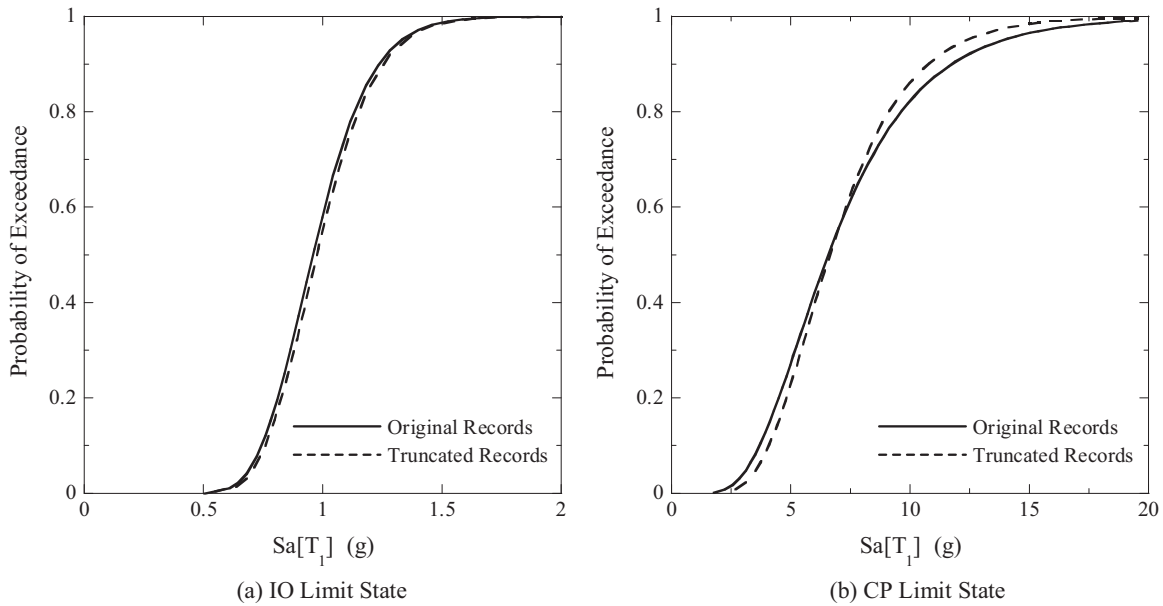


Fig. 3. Fragility curves for 5-story frame based on maximum inter-story drift.

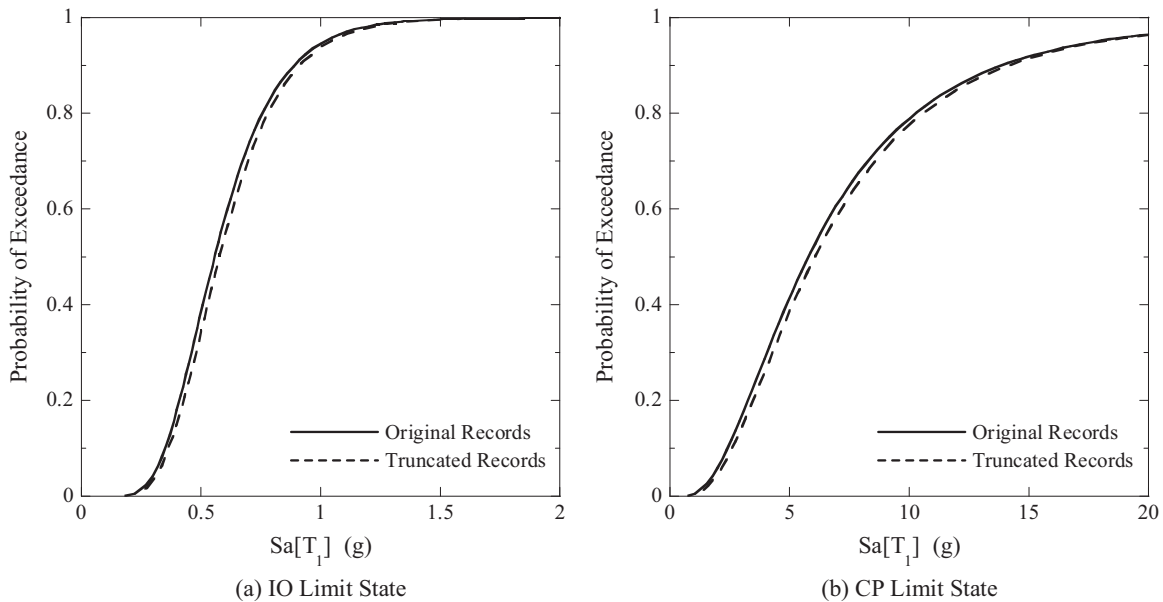


Fig. 4. Fragility curves for 10-story frame based on maximum inter-story drift.

recorded, representing the duration of time over which 90% of the energy is accumulated. Although the total length of the accelerogram may vary depending on the recording device, the 5–95% duration determines the length of the strongest part of the ground motion time history. This duration definition is also independent of the scaling of the record, as the rate of accumulation stays the same, and also does not change with ground motion frequency content. Table 2 presents the earthquake records selected for this study.

4. Incremental dynamics analysis

Of the most prevalent analyses, is Incremental Dynamics Analysis, posed by Vamvatsikos and Cornell [4]. Such an analysis is parametric, which inspects seismic performance of structures when they are under several ground motions. Typical generation

of numerous curves of damage measure versus intensity measure under the effect of several scaled ground motions is its dominant function. 20 appointed ground motion records, as a consequence, were scaled up or down several times.

5. Hazard curve

The seismic hazard curve is plotted using return periods against the magnitude of spectral accelerations at the fundamental structural period ($Sa(T_1)$), considered here as the intensity measure (IM). For a relatively wide range of intensities, the seismic hazard curve can be approximated as a linear function on a log-log scale [22–24] given as follows:

$$\lambda_{Sa(T_1)}(Sa) = k_0(Sa)^{-k} \quad (2)$$

where, $\lambda_{Sa(T_1)}(Sa)$ is the mean annual frequency of $Sa(T_1)$

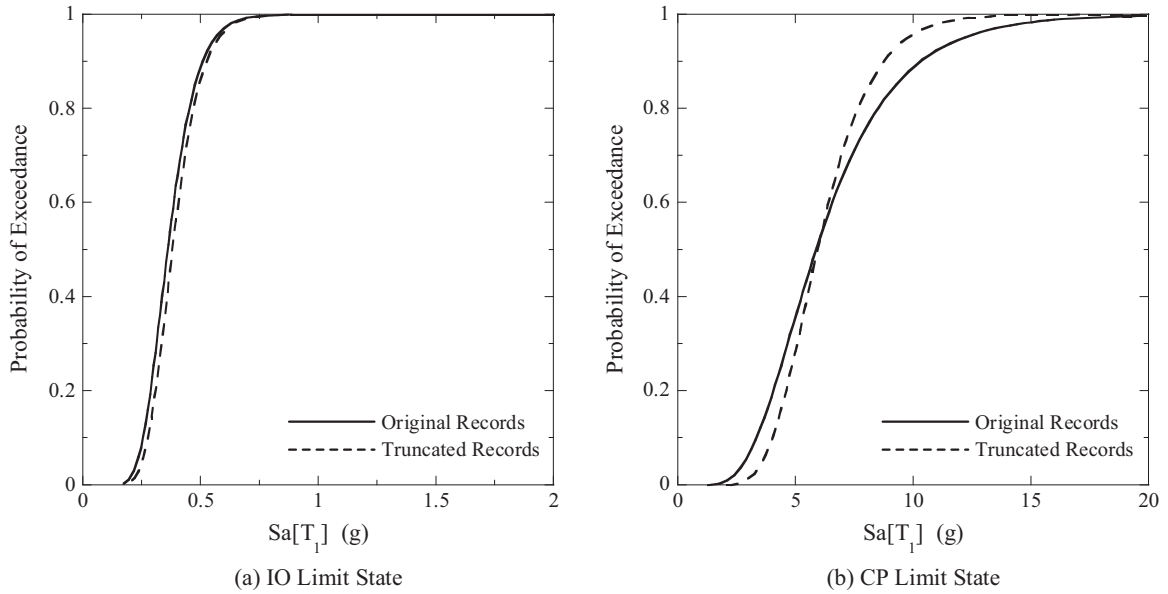


Fig. 5. Fragility curves of 20-story frame based on maximum inter-story drift.

Table 3
Mean Annual Frequency of frames in each limit state and their calculated errors ($\times 10^{-5}$).

Frame		5-story			10-story		20-story	
Maximum inter-story Drift	LS							
	IO							
	CP							
	Original	73.31222	11.93181	296.9205	6.197904	649.5733	2.706145	
	Truncated	71.48838	11.09963	276.5187	5.246692	583.521	2.138782	
	Error (%)	2.487773	6.974499	6.871159	15.34732	10.16856	20.96575	

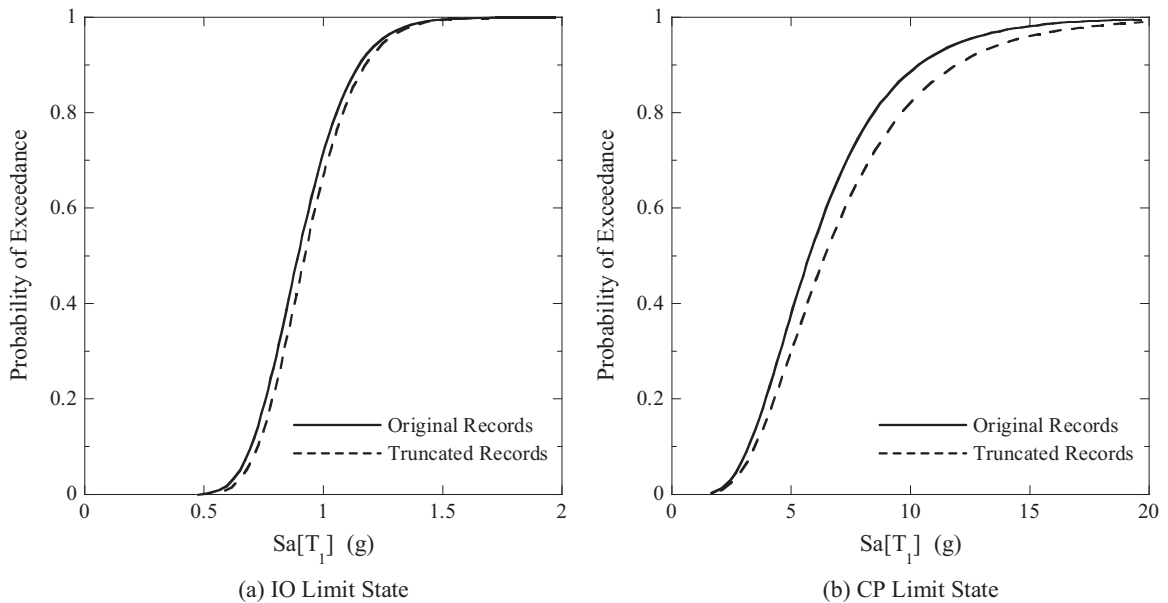


Fig. 6. Fragility curves for 5-story frame based on modified Park & Ang.

exceeding S_a , k and k_0 are the constant coefficients. The average fundamental period of the frames in this study, is about 1.0 second; therefore, the spectral acceleration at the 1-s period is used as the earthquake intensity measure. The seismic hazard curve, shown in Fig. 2, is plotted using the data available in the “Seismic hazard analysis research” conducted by engineering faculty of Tehran University [25] for greater Tehran region. The parameters k_0 and k in Eq. (2), obtained by a regression in the logarithmic plane, are 0.0002 and 1.8633 for the central region of

Tehran, respectively.

Therefore, mean annual frequency (λ_c) can be calculated by this:

$$\lambda_c = \int_{S_a} P(C|Sa(T_1)) \cdot |d\lambda(Sa(T_1))| \tag{3}$$

where $P(C|Sa(T_1))$ is the conditional probability of exceeding the limit state for a given $Sa(T_1)$ and $|d\lambda(Sa(T_1))|$ is the differential of the mean annual frequency of $Sa(T_1)$ exceeding S_a .

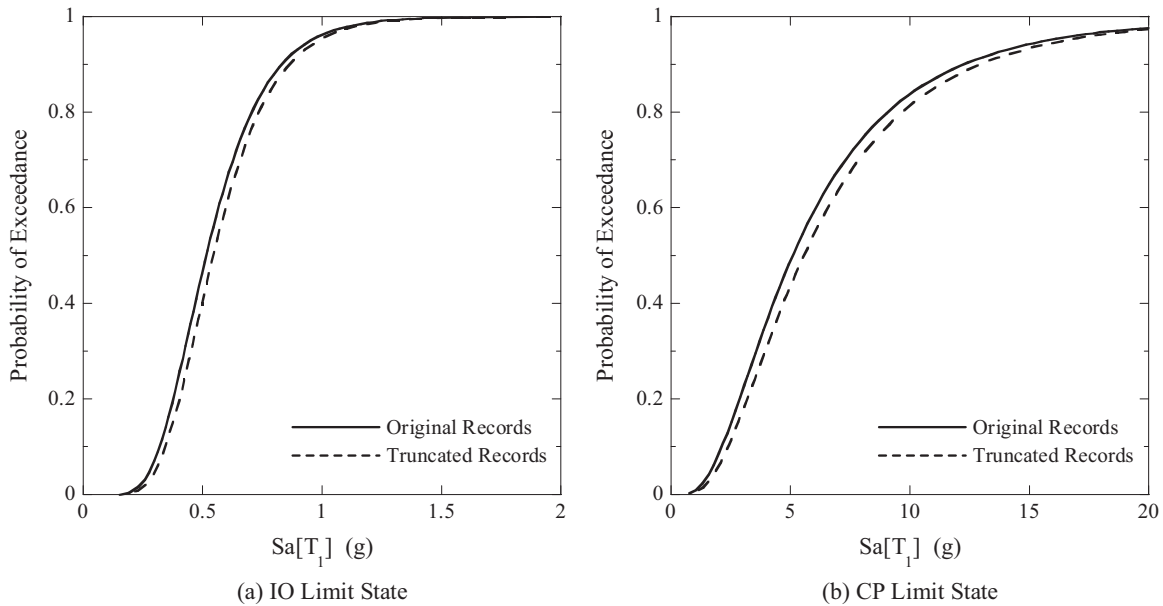


Fig. 7. Fragility curves for 10-story frame based on modified Park & Ang.

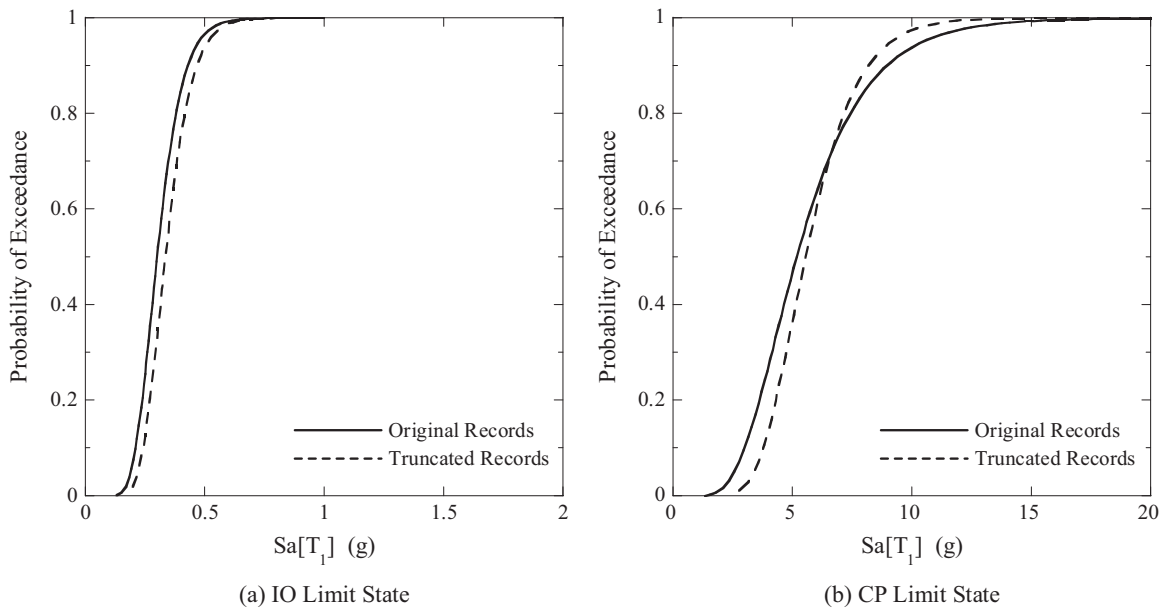


Fig. 8. Fragility curves for 20-story frame based on modified Park & Ang.

Table 4
Mean Annual Frequency of frames in each limit state and their calculated errors ($\times 10^{-5}$).

Frame		5-story		10-story		20-story	
Modified Park & Ang	LS						
	IO						
	CP						
	Original	85.89399	2.874123	356.4401	6.724056	932.8646	3.572684
	Truncated	79.13041	2.483251	312.4981	5.363944	734.4735	2.469992
	Error (%)	7.874329	13.5997	12.32801	20.22755	21.26687	30.86452

6. Damage index and damage limit states

The structural fragility concerning a damage state is clarified as the probability that the structural response exceeds the structural capacity; then, the process of fragility analysis commences with identifying the seismic damage. In the current study, two diverse damage indices were invoked: maximum inter-story drift and modified Park & Ang. Damage limit states for each of them are

discussed hereunder.

For maximum inter-story drift, the yield capacity of the structures or Immediate Occupancy (IO) is identified as being the spectral acceleration point at which the IDA curve leaves the linear path while for the collapse capacity (CP) which is thus not surpassed on the IDA curve until the final point where the local tangent reaches 20% of the elastic slope or $\theta_{max} = 10\%$, whichever occurs first in IM terms.

In this study, the modified Park & Ang damage index is formulated as:

$$DM = \frac{\phi_m - \phi_y}{\phi_u - \phi_y} + \beta_e \cdot \frac{\int dE}{M_y \cdot \phi_u} \quad (4)$$

where, DM=P&A damage index, ϕ_m , ϕ_y and ϕ_u are maximum, yield and ultimate curvatures of the member, respectively; M_y =yield moment; $\int dE$ =total area contained in M- ϕ loops; β_e =Park & Ang empirical factor. For the purpose of calibrating this component, several RC frames are submitted to the incremental dynamic analysis, and the DM value is opted as the one when the structure is tumbled in the nonlinear dynamic analysis. The final value of β_e is the median value of all acquired results [26]. P&A damage index has the potential of being computed in the element, story, and overall scales. In each story, it is calculated in accordance with hysteretic energy weighting factors. The story damage indexes are then totalized with respect to the hysteretic energy of every story to reach the overall damage index of the construction. In this study, $DM \leq 0.1$ is chosen for no damage limit state, $DM=0.2$ is selected for light and $DM = 1$ for collapse limits state of structure; as a result, for $0.1 \leq DM \leq 1$, mean annual exceeding frequency of damage is measured.

7. Fragility curves

The structural fragility is signified as the contingent probability of exceeding the limit state capacity for a stage of ground motion intensity that is given, and fragility curves clearly demonstrate the probability of structural damage in particular limit state for measuring definite intensity. Such curves are typically modeled by a lognormal cumulative distribution function [27]:

$$Fr(x) = \Phi\left(\frac{\ln(x) - \lambda_R}{\xi_R}\right) \quad (5)$$

in which $\Phi[\cdot]$ =standard normal cumulative distribution function, x =intensity measure (i.e., 3-s gust wind speed for tornado fragility curves), λ_R =logarithmic median of capacity R (in units that are dimensionally consistent with demand), and ξ_R =logarithmic standard deviation of capacity R .

8. Results

In this study, fragility curves are used for investigating the accuracy of reducing earthquake record duration. In each damage limit state, Mean Annual Frequency was chosen as seismic criterion for considering the proposed method. Fragility curves were plotted based on maximum inter-story drift and Park-Ang damage indices.

In Figs. 3–5, fragility curves derived by original EQ records are compared with those by truncation of them based on maximum inter-story drift.

According to Fig. 3, it can be concluded that the difference between fragility curves of original EQ records and truncated records is negligible for normal and mid-rise frames on condition that deformation-based indices were chosen. Fragility curves of collapse limit state for 20 story frame show that this difference is more significant by height increase. Mean Annual Frequency of frames and their calculated errors of each limit state, which are shown in Table 3, endorse this assertion.

In Figs. 6–8, fragility curves derived by original EQ records are compared with those by truncation of them based on modified P&A damage index.

It can be seen that differences between fragility curves in each limit state are well more significant than those that are based on maximum inter-story drift. Furthermore, increasing height intensifies them. Likewise before, mean annual frequency approves these results. (Please see Table 4).

9. Conclusion

In order to study the seismic performance of structures more accurately, several ground motions of different intensity level should be considered. To this end, incremental dynamic analysis is an extremely useful method which can become a valuable additional tool for seismic engineering. However, it really takes a lot of time to be done in order to consider the record to record variability and massive study cases. One useful strategy to cope with this problem is earthquake records truncating. In this regard, this study has shown the effects of record truncation on the fragility curves and mean annual frequencies of different RC frames. The fragility curves and MAFs of IO and CP limit states are computed for two different damage indices of interstory drift and the modified Park & Ang. While maximum inter-story drift is based on deformation only, the modified Park & Ang is based on the combination of maximum deformation response and hysteretic energy dissipation. It has been concluded that truncating has little effect on outputs, in the case of normal and mid-rise frames, as long as deformation-based damage indices, like interstory drift, are chosen. On the other hand, investigating seismic performance of structures by energy-based or combination indices are more dependent on the duration of records and truncation may produce more errors. Additionally, high-rise structures with long periods are more sensitive to such changes. Records may be truncated after due consideration of these factors. Based on the computed errors in this study, the truncation effect for IO limit state is less than CP limit state regardless of damage index. Furthermore, this study has shown that more than half the execution time can be saved by truncating the records.

References

- [1] J. Mander, R. Dhakal, N. Mashiko, Incremental dynamic analysis applied to seismic risk assessment of bridges, 2006.
- [2] B. Ferracuti, et al., Verification of displacement-based adaptive pushover through multi-ground motion incremental dynamic analyses, *Eng. Struct.* 31 (8) (2009) 1789–1799.
- [3] C.A. Goulet, et al., Evaluation of the seismic performance of a code-conforming reinforced-concrete frame building—from seismic hazard to collapse safety and economic losses, *Earthq. Eng. Struct. Dyn.* 36 (13) (2007) 1973–1997.
- [4] D. Vamvatsikos, C.A. Cornell, Incremental dynamic analysis, *Earthq. Eng. Struct. Dyn.* 31 (3) (2002) 491–514.
- [5] A. Azarbakht, M. Dolšek, Progressive incremental dynamic analysis for first-mode dominated structures, *J. Struct. Eng.* 137 (3) (2010) 445–455.
- [6] P. Zarfam, M. Mofid, On the modal incremental dynamic analysis of reinforced concrete structures, using a trilinear idealization model, *Eng. Struct.* 33 (4) (2011) 1117–1122.
- [7] D. Vamvatsikos, Performing incremental dynamic analysis in parallel, *Comput. Struct.* 89 (1) (2011) 170–180.
- [8] J. Ruiz-García, On the influence of strong-ground motion duration on residual displacement demands, *Earthq. Struct.* 1 (4) (2010) 327–344.
- [9] I. Iervolino, G. Manfredi, E. Cosenza, Ground motion duration effects on nonlinear seismic response, *Earthq. Eng. Struct. Dyn.* 35 (1) (2006) 21–38.
- [10] M. Raghunandan, A.B. Liel, Effect of ground motion duration on earthquake-induced structural collapse, *Struct. Saf.* 41 (2013) 119–133.
- [11] S. No, 2800, Iranian Code of Practice for Seismic Resistant Design of Buildings, Third Revision, Building And Housing Research Center, Iran, 2005.
- [12] S. SeismoSoft, A computer program for static and dynamic nonlinear analysis of framed structures, 2010.
- [13] J.B. Mander, M.J. Priestley, R. Park, Theoretical stress-strain model for confined concrete, *J. Struct. Eng.* 114 (8) (1988) 1804–1826.
- [14] J.E. Martínez-Rueda, A. Elnashai, Confined concrete model under cyclic load, *Mater. Struct.* 30 (3) (1997) 139–147.
- [15] M. Menegotto, Method of analysis for cyclically loaded RC plane frames

- including changes in geometry and non-elastic behavior of elements under combined normal force and bending, in: Proceedings of the IABSE Symposium on Resistance and Ultimate Deformability of Structures Acted on by Well Defined Repeated Loads, 1973.
- [16] F. Filippou, G. Fenves, *Methods of Analysis for Earthquake-resistant Structures*, CRC, Boca Raton, Fla, 2004.
- [17] M. Fragiadakis, R. Pinho, S. Antoniou, Modelling inelastic buckling of reinforcing bars under earthquake loading, *Computational Structural Dynamics and Earthquake Engineering: Structures and Infrastructures Book Series*, 2010, p. 347.
- [18] FEMA-440, *Improvement of Nonlinear Static Seismic Analysis Procedures*, Federal Emergency Management Agency, 2005.
- [19] J.J. Bommer, A. Martínez-Pereira, The effective duration of earthquake strong motion, *J. Earthq. Eng.* 3 (02) (1999) 127–172.
- [20] M.D. Trifunac, A.G. Brady, A study on the duration of strong earthquake ground motion, *Bull. Seism. Soc. Am.* 65 (3) (1975) 581–626.
- [21] J. Hancock, J.J. Bommer, A state-of-knowledge review of the influence of strong-motion duration on structural damage, *Earthq. Spectra* 22 (3) (2006) 827–845.
- [22] R.T. Sewell, G.R. Toro, R.K. McGuire, *Impact of ground motion characterization on conservatism and variability in seismic risk estimates*, Nuclear Regulatory Commission, Div. Of Engineering Technology; Risk Engineering, Inc, Washington, DC (United States), Boulder, CO (United States), 1996.
- [23] R. Kennedy, S.A. Short, *Basis for Seismic Provisions of DOE-STD-1020*, Lawrence Livermore National Lab., CA United States, Brookhaven National Lab., Upton, NY (United States), RPK Structural Mechanics Consulting, Yorba Linda, CA (United States), EQE International, Inc., San Francisco, CA (United States), 1994.
- [24] C.A. Cornell, Calculating building seismic performance reliability: a basis for multi-level design norms, in: *Proceedings of the 11th World Conference on Earthquake Engineering*, 1996.
- [25] Y. Gholipour, et al., *Probabilistic Seismic Hazard Analysis, Phase I—Greater Tehran Regions. Final Report*, 2008, p. 1.
- [26] M. Ciampoli, *Performance reliability of earthquake-resistant steel-concrete composite structures*, *Sci. Res. Program. Relev. Natl. Interest* (2003).
- [27] F. Jalayer, C.A. Cornell, *A Technical Framework for Probability-Based Demand and Capacity Factor Design (DCFD) Seismic Formats*, Pacific Earthquake Engineering Research Center, 2004.